



CHORUS

This is the accepted manuscript made available via CHORUS. The article has been published as:

Probing molecular spin clusters by local measurements

Filippo Troiani and Matteo G. A. Paris

Phys. Rev. B **94**, 115422 — Published 16 September 2016

DOI: [10.1103/PhysRevB.94.115422](https://doi.org/10.1103/PhysRevB.94.115422)

Probing molecular spin clusters by local measurements

Filippo Troiani*

National Research Center S3 c/o Dipartimento di Fisica via G. Campi 213/A, CNR-INFN, 41100, Modena, Italy

Matteo G. A. Paris[†]

Quantum Technology Lab, Dipartimento di Fisica dell'Università degli Studi di Milano, I-20133 Milano, Italy

(Dated: August 23, 2016)

We address the characterization of molecular nanomagnets at the quantum level and analyze the performance of local measurements in estimating the physical parameters in their spin Hamiltonians. To this aim, we compute key quantities in quantum estimation theory, such as the classical and the quantum Fisher information, in the prototypical case of an heterometallic antiferromagnetic ring. We show that local measurements, performed only on a portion of the molecule, allow a precise estimate of the parameters related to both magnetic defects and avoided level crossings.

PACS numbers: 75.50.Xx, 71.10.Jm, 03.65.Ta

I. INTRODUCTION

Molecular nanomagnets are low-dimensional spin systems, displaying a variety of nonclassical features¹⁻⁵. The magnetic properties of these systems can be interpreted in terms of their spin Hamiltonians, which typically depend on a number of unknown coupling constants^{6,7}. The number of independent parameters can be reduced on the basis of symmetry arguments, and their values can in principle be computed from first-principles^{8,9}. However, these approaches are computationally demanding and are affected by their own uncertainties. Therefore, the parameters entering the spin Hamiltonians are generally obtained by fitting experimental curves^{10,11}.

In particular, when experiments are performed at temperatures lower than the energy gap between ground and first-excited states¹², the estimation of the physical parameters is made possible by the dependence on such quantities of the system ground state¹³. In fact, any variation in some parameter of interest λ modifies the ground state, and thus the statistics related to the accessible physical observables. Any bound to the precision in the estimation procedure should thus be connected to the distance between ground states corresponding to infinitesimally close values of λ ¹⁴⁻¹⁶.

Such intuition can be made more rigorous and quantitative upon employing tools from quantum estimation theory¹⁷⁻²¹. This allows one to design optimal estimation procedures and to compute the fundamental limits to precision, as dictated by quantum mechanics. Indeed, the infinitesimal (Bures) distance between ground states corresponding to neighboring values of λ is proportional to the maximum precision in the estimation of such parameter, achievable by any possible measurement. The connection between the metric structure of the Hilbert space and quantum estimation theory has in fact been exploited to characterize several system of interest in quantum technology and to address quantum critical systems as a resource for quantum estimation²²⁻²⁵.

Here we make use of two key quantities in quantum estimation theory, in order to assess the precision in the estimation of physical parameters entering the spin Hamiltonian of molecular nanomagnets. These quantities are the classical and the quantum Fisher information (FI and QFI, respectively). The

FI provides, through the Cramer-Rao inequality²⁶, a lower bound for the uncertainty in the parameter estimation, based on the statistics of a given observable. The QFI gives an upper bound to the FI of any measurement, and thus the best possible precision in the estimation allowed by quantum mechanics, for a given parametric dependence of the system (ground) state. In this way, benchmarks for either local or global quantum measurements can be obtained, and exploited to assess and compare different classes of detection techniques. As a matter of fact, quantum estimation theory also provides tools to identify the optimal observable, i.e. the observable whose FI equals the QFI, thus paving the way for possible practical implementations.

We address the characterization of molecular nanomagnets at the quantum level and analyze the performances of local measurements, realized by addressing a portion of the entire compound, as opposed to global ones, requiring access to the molecule as a whole. Our results clearly indicate that fluctuations induced by the total-spin and magnetization tunneling at a level anticrossing, or by the introduction of a magnetic defect, can be monitored locally, with nearly the ultimate precision allowed by quantum mechanics. Overall, we provide quantitative results on precision bounds that are applicable to general classes of measurements.

The paper is structured as follows. In Section II we set notation and introduce the basic tools of quantum estimation theory. In Section III we analyze estimation problems where the ground-state dependence at avoided level crossings is relevant, whereas in Section IV we address estimation of parameters related to a magnetic defect. Section V closes the paper with some concluding remarks.

II. THEORETICAL BACKGROUND

We consider a spin Hamiltonian \mathcal{H} , which depends on an unknown parameter λ . The value of λ has to be inferred by performing quantum-limited measurements on the system ground state $|\psi_\lambda\rangle$, and by suitably processing the sample of experimental data. The inferred value of the unknown parameter can thus be expressed as a function of such data, known

as the *estimator*, and typically denoted with $\hat{\lambda}$. This is said to be *unbiased* if its expectation value coincides with the actual value of the parameter λ . For a given observable, an unbiased maximum-likelihood estimator $\hat{\lambda}$ allows to saturate the classical Cramer-Rao bound. The fundamental limit to the precision that can be achieved, through an arbitrary observable, in the estimate of λ is instead given by the quantum Cramer-Rao bound: $1/\text{Var}(\hat{\lambda}) \leq H(\lambda)$, where $H(\lambda)$ is the quantum Fisher information and $\text{Var}(\hat{\lambda})$ is the variance of any unbiased estimator, corresponding to the average square distance between λ and $\hat{\lambda}$. For a pure state, the QFI is given by

$$H(\lambda) = 4 [\langle \partial_\lambda \psi_\lambda | \partial_\lambda \psi_\lambda \rangle + |\langle \partial_\lambda \psi_\lambda | \psi_\lambda \rangle|^2] \\ = 4 \left[\sum_k |\partial_\lambda c_k|^2 + |c_k^* (\partial_\lambda c_k)|^2 \right]. \quad (1)$$

Here the ground state is expanded in a parameter-independent basis, $|\psi_\lambda\rangle = \sum_k c_k(\lambda) |k\rangle$, such that $|\partial_\lambda \psi_\lambda\rangle = \sum_k (\partial_\lambda c_k) |k\rangle$.

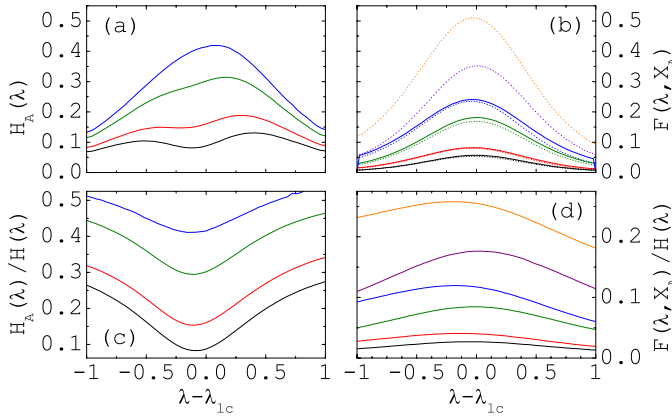


FIG. 1: (Color online) Quantum estimation of the Cr_7Ni molecule ground state at the anticrossing. We show results for measurements performed on different subsystems A of the ring ($\alpha/\Delta = 1$), formed by the first n_A consecutive spins, with $n_A = 2$ (black curves), 3 (red), 4 (green), 5 (blue), 6 (purple), and 7 (orange) respectively. The four panels show: (a) the QFI; (b) the FI corresponding to the observable $X_A \equiv \rho_{11}^A - \rho_{22}^A$ (dotted lines), and QFI obtained for a mixture of the diabatic states (solid lines); the (c) QFI and (d) FI of the subsystems, normalized to the QFI of the whole ground state. The dotted lines in (b) represent the QFI corresponding to the mixture, rather than the linear superposition, of the states $|1\rangle$ and $|2\rangle$.

If only a specific observable X is available, then the precision of the parameter estimation is bounded by the classical Cramer-Rao inequality: $1/\text{Var}(\hat{\lambda}) \leq F(\lambda, X)$. Here

$$F(\lambda, X) = \sum_x p_\lambda(x) [\partial_\lambda \ln p_\lambda(x)]^2 = \sum_x \frac{[\partial_\lambda |\langle x | \psi_\lambda \rangle|^2]^2}{|\langle x | \psi_\lambda \rangle|^2} \quad (2)$$

is the Fisher information, and $p_\lambda(x) = |\langle x | \psi_\lambda \rangle|^2$ is the probability of obtaining the outcome x from the measurement of X , at a given λ . The quantum Cramer-Rao theorem states that the

FI is bounded from above by the QFI: $F(\lambda, X) \leq H(\lambda)$. Any observable X which saturates the above inequality is said to be *optimal*, in that it maximizes the precision in the estimate of λ .

The optimal measurement generally involves accessing the system ground state as a whole. A question arises on whether, and to which extent, its performances can be emulated by measurements that are local in nature, i.e. performed only on a portion of the entire system. Such question can be answered by evaluating the QFI for the reduced density operator describing a specific subsystem A , as obtained by performing a partial trace on the complementary subsystem B , $\rho_\lambda^A = \text{Tr}_B [|\psi_\lambda\rangle\langle\psi_\lambda|]$. The local QFI is given by the expression

$$H_A(\lambda) = 2 \sum_{i,j} \frac{|\langle \phi_i | \partial_\lambda \rho_\lambda^A | \phi_j \rangle|^2}{p_i + p_j}. \quad (3)$$

Here, p_i and $|\phi_i\rangle$ are the eigenvalues and eigenstates of ρ_λ^A , respectively, and the sum is extended over all the indices such that $p_i + p_j > 0$.

The above quantities allow a thorough characterization of the parameter estimation performed through measurements on the system ground state. In fact, the ratio between FI and QFI quantifies the relative suitability of the observable X to estimate the parameter λ . The ratio H_A/H , instead, assesses to which extent a precise estimate of λ can be obtained by means of local measurements within a given subsystem A .

III. LEVEL ANTICROSSINGS

In analyzing the ground-state dependence on a physical parameter, a special attention should be devoted to the avoided level crossings. Here, small variations of a physical parameter can induce large changes in the system ground state, which are reflected in pronounced peaks of the QFI and, possibly, of the FI of some accessible observable. Level anticrossings thus represent a resource for the characterization of spin Hamiltonians. For the sake of the following discussion, we write the spin Hamiltonian in the generic form $\mathcal{H} = \mathcal{H}_0 + \lambda \mathcal{H}_1 + \mathcal{H}_2$, where the two dominant terms \mathcal{H}_0 and \mathcal{H}_1 commute with each other, but not with the small term \mathcal{H}_2 . By varying the parameter λ in the vicinity of some critical value λ_{lc} , one can induce a level crossing between two joint eigenstates of \mathcal{H}_0 and \mathcal{H}_1 , hereafter denoted by $|1\rangle$ and $|2\rangle$. If these two states are energetically far from all the others for $\lambda \simeq \lambda_{lc}$, the system Hamiltonian can be projected on a two-dimensional subspace and thus reduced to

$$h = \frac{1}{2} [-\alpha(\lambda - \lambda_{lc})\sigma_3 + \Delta\sigma_1], \quad (4)$$

where $\alpha = \langle 2 | \mathcal{H}_1 | 2 \rangle - \langle 1 | \mathcal{H}_1 | 1 \rangle$ is the rate with which the diagonal gap varies as a function of λ and $\Delta = 2\langle 1 | \mathcal{H}_2 | 2 \rangle$ is assumed to be real and positive. The operators σ_j ($j = 1, 3$) are Pauli matrices in the basis $\{|1\rangle, |2\rangle\}$. The ground state of such effective two-level system can be written as $|\psi_\lambda\rangle =$

$c_1(y)|1\rangle + c_2(y)|2\rangle$, where

$$c_1 = \frac{(y + \sqrt{1+y^2})^{1/2}}{\sqrt{2}(1+y^2)^{1/4}}, \quad c_2 = -(1-c_1^2)^{1/2}, \quad (5)$$

and $y \equiv \alpha(\lambda - \lambda_{lc})/\Delta$ represents the (normalized) distance of the parameter λ from the critical value λ_{lc} . It follows that the FI corresponding to a generic observable X can be written in the product form $F = (\alpha/\Delta)^2 f_X(y)$, where the function f_X is given by the following expression:

$$f_X = \frac{y + \sqrt{1+y^2}}{2(1+y^2)^{5/2}} \sum_x \left\{ \frac{\langle 1|x \rangle^2 - \langle 2|x \rangle^2 + 2y\langle 1|x \rangle\langle 2|x \rangle}{[y + \sqrt{1+y^2}]\langle 1|x \rangle - \langle 2|x \rangle} \right\}^2. \quad (6)$$

In fact, also the quantum Fisher information can be written in a factorized form:

$$H = \frac{(\alpha/\Delta)^2}{\{1 + [\alpha(\lambda - \lambda_{lc})/\Delta]^2\}^2} \equiv (\alpha/\Delta)^2 f_H(y). \quad (7)$$

The above functions f_X and f_H thus specify the dependence of the highest precision achievable in the parameter estimation on the distance y from the crossing point. The presence of the prefactor $(\alpha/\Delta)^2$ quantifies the increase of the precision that can be achieved, for each given distance y , by making the anticrossing narrower.

From the above expressions of the FI and QFI it follows that an observable X is optimal if there are two measurement outcomes x and x' allowing for a perfect discrimination between any two orthogonal states. In other words, $|x\rangle$ and $|x'\rangle$ must be orthogonal linear superpositions of the states $|1\rangle$ and $|2\rangle$ alone, or, equivalently, there must be no finite matrix element $\langle i|X|j\rangle$, with $|i| \leq 2\rangle$ and $|j| > 2\rangle$ eigenstates of $\mathcal{H}_0 + \mathcal{H}_1$. In this case, in fact, $f_X(y) = f_H(y)$, and the FI of X equals the QFI. It can be easily verified that (in the absence of degeneracy at the distance y of interest) both \mathcal{H}_0 and \mathcal{H}_1 fulfill the above condition, and thus represent optimal observables.

We finally consider the role of the phase coherence between the two states $|1\rangle$ and $|2\rangle$ by comparing the FI and QFI of $|\psi_\lambda\rangle$ with those obtained for the mixture $\sigma_\lambda = c_1^2|1\rangle\langle 1| + c_2^2|2\rangle\langle 2|$. The QFI of the mixture σ_λ can be shown to coincide with that of the linear superposition $|\psi_\lambda\rangle$ ($f_H^{inc} = f_H$). On the other hand, the expression of the FI is different in the two cases, being

$$f_X^{inc} = \frac{y + \sqrt{1+y^2}}{2(1+y^2)^{5/2}} \sum_x \frac{(\langle 1|x \rangle^2 - \langle 2|x \rangle^2)^2}{[(y + \sqrt{1+y^2})\langle 1|x \rangle]^2 + \langle 2|x \rangle^2}. \quad (8)$$

It can be easily verified that, in the presence of a mixture, an observable X allows an optimal parameter estimation at the anticrossing ($f_X^{inc} = f_H^{inc}$) only if it has $|1\rangle$ and $|2\rangle$ as eigenstates. Therefore, the highest precisions that can be achieved in the presence of a mixture and of a linear superposition coincide, but the conditions on the optimal observables X are more restrictive in the former case. Further details on the derivation of the above equations can be found in the Appendix A.

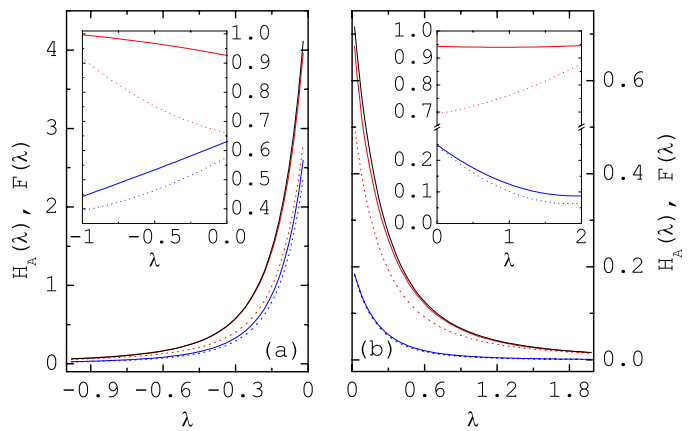


FIG. 2: (Color online) Quantum estimation of the exchange coupling between the magnetic defect and the neighboring spins (Cr-Ni), with respect to that between all the other neighboring spins (Cr-Cr). QFI (solid curves) and FI (dotted) corresponding to two- (blue) and three-spin (red) subsystems. Panels (a) and (b) correspond to ferromagnetic and antiferromagnetic Cr-Ni coupling, respectively. In the insets of the two panels, the same quantities are normalized to the QFI of the whole ground state.

A. Numerical results

The problem of estimating the physical parameters that enter the spin Hamiltonian is ubiquitous in molecular magnetism. In the following, we consider in some detail the representative example of the Cr_7Ni molecule. Its magnetic core is formed by seven Cr^{3+} ions, each carrying an $s_{\text{Cr}} = 3/2$ spin, and one Ni^{2+} ion, with $s_{\text{Ni}} = 1^{27}$. As a spin ring with dominant antiferromagnetic exchange interaction, Cr_7Ni represents a prototypical model of a highly-correlated, low-dimensional quantum system²⁸. Besides, the presence in such molecule of the Ni ion allows us to extend the present discussion to the role of magnetic defects. Given the purpose of the present paper, we focus on the functional dependence of the FI and QFI on the main physical parameters entering the spin Hamiltonian, rather than on their specific values, as estimated by different experimental and theoretical means.

As an example of an anticrossing in the system ground state, we consider the one between the lowest eigenstates of $\mathcal{H}_0 + \mathcal{H}_1$ with $S = M = 1/2$ and $S = M = 3/2$, hereafter labeled $|1\rangle$ and $|2\rangle$, respectively. The above two terms of the Hamiltonian account for the exchange interaction between neighboring spins, $\mathcal{H}_0 = J \sum_{k=1}^8 \mathbf{s}_k \cdot \mathbf{s}_{k+1}$ (with $J > 0$), and for the coupling to an applied magnetic field, $\mathcal{H}_1 = -\lambda \alpha S_z$. The unknown parameter λ thus coincides with the Zeeman splitting in units of α , and can be identified for example with the g -factor of the molecule for $\alpha = \mu_B B$. The zero-field gap between the ground $S = 1/2$ doublet and the lowest $S = 3/2$ quadruplet, mainly induced by the exchange interaction, determines the value of λ_{lc} . The small term \mathcal{H}_2 includes all the remaining contributions in the spin Hamiltonian, which are responsible for the gap Δ^{27} .

The dependence on λ of the system ground state and of the

corresponding reduced density operators is summarized by the behavior of the FI and of the QFI. In particular, three main features emerge from the $H_A(\lambda)$. First, for subsystems A formed by a small number of consecutive spins ($n_A = 2, 3, 4$), the highest values of H_A are obtained away from the crossing point, where the QFI presents instead a clear dip [see Fig. 1(a)]. Second, such feature can be linked to the phase coherence between the states $|1\rangle$ and $|2\rangle$ that contribute to the ground state $|\psi_\lambda\rangle$. In fact, the value of the QFI corresponding to the mixture $\sigma_\lambda^A = c_1^2(y)\rho_{11}^A + c_2^2(y)\rho_{22}^A$, with $\rho_{ij}^A = \text{Tr}_B(|i\rangle\langle j|)$, presents lower values for all λ s, and a maximum close to $\lambda = \lambda_{lc}$ [solid lines in Fig. 1(b)]. The QFI of σ_λ^A also corresponds to the maximum of the FI of $|\psi_\lambda\rangle$, restricted to observables X that are diagonal in the basis of the diabatic states $\{|1\rangle, |2\rangle\}$. Therefore, the comparison between the QFI of ρ_λ^A and σ_λ^A shows that the performance of a local observable X at an avoided level crossing can in general benefit from the fact that X is not diagonal in the basis of the diabatic states. Third, within the diagonal observables, the operator $X_A \equiv \rho_{11}^A - \rho_{22}^A$ (dotted lines) is approximately optimal. Finally, we note that not only the maximum of the QFI of local observables can be localized away from the crossing point, but λ_{lc} also corresponds to an absolute minimum for the relative suitability of the local measurements. This clearly emerges from the plots of $H_A(\lambda)$ and $F(\lambda, X_A)$, normalized to the QFI of the ground state [Fig. 1(c,d)].

In order to gain some quantitative insight into the problem, we consider the case where the actual value of the unknown parameter $\lambda = g$ is 2, and this coincides with the critical value, given the applied magnetic field B . In this case, the mean squared error in the estimate of the g -factor resulting from a single quantum measurement is given by $\text{Var}^{1/2}(\hat{\lambda}) = (\Delta/\mu_B B)[H_A(y=0)]^{-1/2}$, which for two spins (black curves), is approximately 0.05 (we have taken $B = 10$ T, which approximately corresponds to the field that induces the level crossing between the $S = M = 1/2$ and the $S = M = 3/2$ eigenstates, and $\Delta = 0.1$ K, which is a typical value of the gap in the Cr-based rings). The mean squared error can in principle be reduced by a factor \sqrt{N} by passing from a single measurement to a set of N measurements, or by working at a narrower anticrossing. A few details on the numerical calculation of the Hamiltonian eigenstates are provided in Appendix B.

IV. ESTIMATING PARAMETERS RELATED TO A MAGNETIC DEFECT

We next consider a ground state that changes gradually with λ , away from a level crossing (here, \mathcal{H}_0 and \mathcal{H}_1 don't commute, and \mathcal{H}_2 can be set to zero). In particular, we are interested in the case where the unknown parameter is related to a magnetic defect, such as the $s_8 = s_{\text{Ni}}$ spin in the Cr_7Ni molecule. This spin represents a defect because its length differs from that of all the other spins in the ring. Besides, the Cr-Ni exchange coupling can differ from the Cr-Cr ones, and the Ni g -factor can differ from that of the Cr ions.

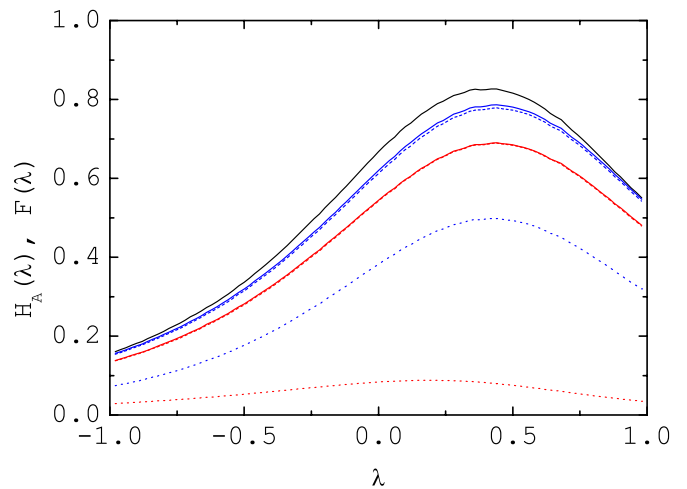


FIG. 3: (Color online) Quantum estimation of the inhomogeneity in the g -factor associated with the magnetic defect, i.e. $\mu_B(g_{\text{Ni}} - g_{\text{Cr}})B/J$. Solid curves correspond to the QFI: for the whole system (black), for subsystems formed by two (red) or three spins (blue). Dashed and dotted curves correspond to the FI for the local magnetization, with and without resolution between the spins of the subsystem.

A. Exchange interaction

We start by considering the effect of an inhomogeneous exchange interaction, and correspondingly group the relevant part of the spin Hamiltonian into the two terms:

$$\mathcal{H}_0 = J \sum_{k=1}^6 \mathbf{s}_k \cdot \mathbf{s}_{k+1}, \quad \mathcal{H}_1 = \lambda J s_8 \cdot (\mathbf{s}_7 + \mathbf{s}_1), \quad (9)$$

where the unknown parameter λ coincides with the ratio between the Cr-Ni and Cr-Cr exchange couplings.

The dependence of the system ground state on λ is characterized in terms of the QFI $H(\lambda)$ (Fig. 2), both for negative and positive values of the parameter [panels (a) and (b), respectively]. For $\lambda < 0$, the defect is ferromagnetically coupled to its neighbors, and the system ground state has $S = 5/2$. For $\lambda > 0$, instead, such coupling is antiferromagnetic, and the total spin is $S = 1/2$. In both cases, $H(\lambda)$ is maximal for $\lambda \rightarrow 0$, and decreases monotonically with $|\lambda|$ (solid black curves). The distinguishability between two (infinitesimally) close values of λ is thus relatively large in the weak-coupling limit, while the ground state is weakly dependent on the precise value of λ in the (more realistic) range of values $\lambda \simeq 1$. In the considered range of parameters, the lowest mean squared error that can be achieved in the estimate of the Cr-Ni exchange coupling by means of a single quantum measurement, $\text{Var}^{1/2}(\hat{\lambda}) = J[H(\lambda)]^{-1/2}$, is of the order of the Cr-Cr exchange coupling J . Besides the absolute value of the QFI, we are interested here in the comparison between the QFI corresponding to the ground state and the same quantity derived for the reduced density operators. We note that, already for subspaces A formed by three consecutive spins (solid red), $H_A(\lambda)$ approaches $H(\lambda)$. The QFI

corresponding to two-spin subsystem (solid blue), instead, approaches $H(\lambda)$ only for $\lambda < 0$. The ratios between the local QFI and that of the whole ground state are reported in the figure insets. Therefore, local observables are in principle well suited for precisely estimating the exchange coupling between the magnetic defect and the neighboring spins. Interestingly, local observables consisting of exchange operators, $X(n_A) = \sum_{i=k}^{k+n_A-1} \mathbf{s}_i \cdot \mathbf{s}_{i+1}$, are nearly optimal. This is shown by the FI corresponding to $n_A = 2$ and $n_A = 3$ (dotted curves), which are very close to the QFI of the corresponding subsystems. The Fisher information of the local magnetization (not shown) gives instead significantly lower values.

B. Zeeman coupling

The magnetic defect affecting the ground state can also consist in the presence of a spin with a different g -factor (or, equivalently, in a local magnetic field). In this case, the relevant terms of the spin Hamiltonian are grouped as follows:

$$\mathcal{H}_0 = J \sum_{k=1}^8 \mathbf{s}_k \cdot \mathbf{s}_{k+1}, \quad \mathcal{H}_1 = \lambda J s_{N,z}. \quad (10)$$

The unknown parameter λ thus corresponds to the difference in the Zeeman splitting of the Ni ion with respect to that of the Cr ions, normalized to the exchange coupling, $\lambda = \mu_B(g_{\text{Ni}} - g_{\text{Cr}})B/J$. The quantum Fisher information of the system ground state (solid black line in Fig. 3) presents a pronounced maximum for $\lambda \simeq 0.5$. As in the previous case, the QFI information corresponding to two- and three-spin subsystems (solid blue and red, respectively) approaches $H(\lambda)$, especially if the subsystems A includes the defect. The FI corresponding to the local magnetization, $X(n_A) = \sum_{i=k}^{k+n_A} a_i s_{i,z}$, falls significantly below the QFI for the corresponding subsystem if the observable is not spin selective ($a_i = a_j$ for all $i \neq j$, dotted lines). However, if the magnetization is spin selective ($a_i \neq a_j$ for $i \neq j$, dashed lines), the values of the FI are very close to the maximal ones. In the latter case, the magnetization thus represents a nearly optimal observable for the parameter estimation.

V. CONCLUSIONS

We have analyzed the performances of local measurements in estimating different physical parameters that enter the spin Hamiltonian of a molecular nanomagnet. Local measurements are shown to allow a precise estimation of parameters related to both magnetic defects and avoided level crossings. Parameters such as the exchange coupling or the g -factor of a magnetic defect can be estimated locally —with nearly the ultimate precision allowed by quantum mechanics— by measuring related observables, namely the exchange operators and the local magnetization, respectively. Local measurements also approach the ultimate precision in the parameter estimation at avoided level crossings, where the commutation relations between the observable and the Hamiltonian are shown

to play a relevant role. Our results clearly show the effectiveness of local measurements in probing Hamiltonian parameters, thus paving the way for the development of optimal characterization schemes for molecular spin clusters.

Acknowledgements

This work was funded by: the Italian Ministry of Education and Research, through the FIRB project RBFR12RPD1 and the Progetto Premiale EOS; the US AFOSR/AOARD program (contract FA2386-13-1-4029); the EU, through the Collaborative Projects QuProCS (Grant Agreement 641277) and the FP7 FET project *MoQuaS* (contract N.610449); the UniMI, through the H2020 Transition (Grant 14-6-3008000-625).

APPENDIX A: DERIVATION OF THE ANALYTICAL RESULTS

The ground state $|\psi_\lambda\rangle$ of the effective Hamiltonian h in Eq. (4) can be expressed as a function of the basis states $|1\rangle$ and $|2\rangle$ by means of the coefficients

$$c_1(y) = P(y)Q(y), \quad c_2(y) = -Q(y), \quad (11)$$

where $y = \alpha(\lambda - \lambda_c)/\Delta$ is the normalized distance of the parameter λ from the critical value. The functions P and Q are given by the following expressions:

$$P(y) = y + \sqrt{1 + y^2}, \quad Q^{-1}(y) = \sqrt{2P(y)}(1 + y^2)^{1/4}. \quad (12)$$

From the above equations, it follows that the derivatives of the coefficients, entering the expressions of both the classical and the quantum Fisher information, are given by:

$$\partial_y c_1(y) = \frac{Q(y)}{2(1 + y^2)}, \quad \partial_y c_2(y) = \frac{P(y)Q(y)}{2(1 + y^2)}. \quad (13)$$

As a result, the expression of $H(\lambda)$ takes the form:

$$H = 4(\alpha/\Delta)^2 [(\partial_y c_1)^2 + (\partial_y c_2)^2] = \frac{(\alpha/\Delta)^2}{(1 + y^2)^2}, \quad (14)$$

where we made use of the equation $\partial_\lambda = (\alpha/\Delta)\partial_y$. As to the classical Fisher information corresponding to the observable X , this can be written as a function of the amplitudes $\langle 1|x\rangle$ and $\langle 2|x\rangle$ (which are assumed to be real, for simplicity), of the coefficients c_1 and c_2 , and of their derivatives with respect to λ (or y). These enter the expression of the probabilities

$$p_\lambda(x) = \langle \psi_\lambda | x \rangle^2 = \sum_{k,l=1}^2 c_k(y)c_l(y)\langle k|x\rangle\langle x|l\rangle. \quad (15)$$

The derivative of such probability with respect to y can be shown to be:

$$\partial_y p_\lambda(x) = \frac{P(y)[Q(y)]^2}{1 + y^2} (\langle 1|x\rangle^2 - \langle 2|x\rangle^2 + 2y\langle 1|x\rangle\langle 2|x\rangle). \quad (16)$$

After replacing the two above expressions into that of the Fisher information,

$$F(\lambda, X) = (\alpha/\Delta)^2 \sum_x \frac{[\partial_y p_\lambda(x)]^2}{p_\lambda(x)}, \quad (17)$$

one can derive the Eq. (6) reported in the manuscript.

In order to highlight the role of the phase coherence between the two basis states, the QFI of $|\psi_\lambda\rangle$ can be compared with that obtained for the statistical mixture of $|1\rangle$ and $|2\rangle$, with populations corresponding to $[c_k(y)]^2$. In this case, the probabilities $p_\lambda(x)$ take the form

$$p_\lambda^{inc}(x) = \sum_{k=1}^2 [c_k(y)\langle k|x\rangle]^2. \quad (18)$$

The corresponding derivative with respect to y reads

$$\partial_y p_\lambda^{inc}(x) = \frac{P(y)[Q(y)]^2}{1+y^2} (\langle 1|x\rangle^2 - \langle 2|x\rangle^2). \quad (19)$$

The adimensional function that enters the expression of the quantum Fisher information thus becomes the one reported in Eq. (8). This also corresponds to the function f_X for an observable $X = \sum_x x|x\rangle\langle x|$, which is diagonal in the basis of the diabatic states, and thus such that $\langle 1|x\rangle\langle x|2\rangle = 0$ for any x . This follows simply from the fact that, for such an observable, $p_\lambda(x) = p_\lambda^{inc}(x)$.

We next consider the case where there are two outcomes of the measurement of X , x and x' , with corresponding eigenstates $|x\rangle$ and $|x'\rangle$ that are mutually orthogonal and belong to the two-dimensional subspace $\{|1\rangle, |2\rangle\}$. We write them as linear combinations of the basis states, with real coefficients (what follows can be easily generalized to the case of complex coefficients): $|x\rangle = a|1\rangle + b|2\rangle$ and $|x'\rangle = b|1\rangle - a|2\rangle$. Plugging these expressions into the Eq. (1) of the manuscript, one obtains, after some algebra, the equation $f_X = f_H = 1/(1+y^2)^2$, which implies that the measurement is optimal.

In the case of the Cr₇Ni ring, the observable $X_A \equiv \rho_{11}^A - \rho_{22}^A$ is diagonal in the basis of the states $|1\rangle$ and $|2\rangle$ (even if it doesn't belong to the two-dimensional subspace). In fact, $|1\rangle$ and $|2\rangle$ are eigenstates of S_z , corresponding to different values, $M_1 = 1/2$ and $M_2 = 3/2$, of the total spin projection. The reduced density operators ρ_{kk}^A (and thus X_A) can be written as mixtures of density operators, each with a defined value of the total spin projection. This follows from

the fact that each finite term of ρ_{kk}^A comes from contributions like $\langle i_B|k\rangle\langle k|i_B\rangle$, with $|i_B\rangle$ a basis state of the subsystem B , which can be chosen so as to have a defined value of the spin projection M_B . The ket and the bra in the term of ρ_{kk}^A thus have to be characterized by the same value of $M_A = M_k - M_B$. As a result, $\rho_{kk}^A \otimes I_B$ cannot have matrix elements between states with different values of the total spin projection, such as $|1\rangle$ and $|2\rangle$.

APPENDIX B: NUMERICAL CALCULATIONS

The eigenstates of Cr₇Ni are obtained by numerically diagonalizing the Hamiltonian, with the inclusion of the exchange and of the Zeeman terms. The Hamiltonian is computed and diagonalized within the irreducible tensor operator formalism¹¹. In the case of the avoided level crossing, the Hamiltonian commutes with \mathbf{S}^2 and S_z , and can be diagonalized independently within each (S, M) subspace, with $S = M = 1/2$ (dimension 574) and $S = M = 3/2$ (dimension 1000). The eigenstates are the expanded in a local basis $|m_1, m_2, \dots, m_8\rangle$ (with m_i the projection of the i -th spin along z), and the terms ρ_{ij}^A are computed by performing a partial trace over the spins that don't belong to the subsystem of interest A . The reduced density operators ρ_λ is then computed by combining the above operators, through the expression $\rho_\lambda^A = \sum_{i,j=1}^2 c_i(\lambda)c_j(\lambda)\rho_{ij}^A$. This matrix is diagonalized numerically, for all the values $\lambda_k = k\delta\lambda$ of the parameter λ in the grid, so as to obtain the eigenvalues p_i and the eigenvectors $|\phi_i\rangle$ that enter the expression of H_A , for each point of the grid. The derivative of the reduced density operator, $\partial_\lambda \rho_\lambda^A$, is computed numerically as $(\rho_{\lambda_{k+1}}^A - \rho_{\lambda_{k-1}}^A)/(2\delta\lambda)$.

The introduction of the magnetic defect reduces the symmetry of the Hamiltonian. In particular, in the case of the exchange coupling the ground state of the spin Hamiltonian belongs either to the $S = 5/2$ or to the $S = 1/2$ subspaces, depending on whether the Cr-Ni coupling is ferromagnetic or antiferromagnetic, respectively. In the case of the magnetic field, \mathcal{H}_1 doesn't commute with \mathbf{S}^2 . This implies that the ground state has to be calculated in a larger subspace, including all the basis states with total spin from $1/2$ to $S_{max} > 1/2$. The value of S_{max} is determined upon convergence of the ground state energy and depends on the value of λ .

* Electronic address: troiani.filippo@unimore.it

† Electronic address: matteo.paris@fisica.unimi.it

¹ J. R. Friedman, M. P. Sarachik, J. Tejada, and R. Ziolo, Phys. Rev. Lett. **76**, 3830 (1996).

² W. Wernsdorfer, R. Sessoli, Science **284**, 133 (1999).

³ A. Ardavan, O. Rival, J. J. L. Morton, S. J. Blundell, A. M. Tyryshkin, G. A. Timco, and R. E. P. Winpenny, Phys. Rev. Lett. **98**, 057201 (2007).

⁴ C. Schlegel, J. van Slageren, M. Manoli, E. K. Brechin, and M.

Dressel, Phys. Rev. Lett. **101**, 147203 (2008).

⁵ S. Bertaina, S. Gambarelli, T. Mitra, B. Tsukerblat, A. Müller, and B. Barbara, Nature (London) **453**, 203 (2008).

⁶ D. Gatteschi, R. Sessoli, J. Villain, *Molecular nanomagnets* (Oxford University Press, Oxford, 2007).

⁷ A. Furrer and O. Waldmann, Rev. Mod. Phys. **85**, 367 (2013).

⁸ V. Bellini, G. Lorusso, A. Candini, W. Wernsdorfer, T. B. Faust, G. A. Timco, R. E. P. Winpenny and M. Affronte, Phys. Rev. Lett. **106**, 227205 (2011).

- ⁹ M. F. Islam, J. F. Nossa, C. M. Canali, and M. Pederson, Phys. Rev. B **82**, 155446 (2010).
- ¹⁰ J. Schnack and M. Luban, Phys. Rev. B **63**, 014418 (2000).
- ¹¹ E. Livioviti, S. Carretta, and G. Amoretti J. Chem. Phys. **117**, 3361 (2002).
- ¹² E. Micotti, Y. Furukawa, K. Kumagai, S. Carretta, A. Lascialfari, F. Borsa, G. A. Timco, and R. E. P. Winpenny, Phys. Rev. Lett. **97**, 267204 (2006).
- ¹³ M. G. A. Paris, J. Phys. A **49**, 03LT02 (2016).
- ¹⁴ P. Zanardi, N. Paunković, Phys. Rev. E **74**, 031123 (2006).
- ¹⁵ M. Cozzini, P. Giorda, P. Zanardi, Phys. Rev. B **75**, 014439 (2007).
- ¹⁶ P. Zanardi, P. Giorda, M. Cozzini, Phys. Rev. Lett. **99**, 100603 (2007).
- ¹⁷ C. W. Helstrom, *Quantum Detection and Estimation Theory* (Academic Press, New York, 1976); A.S. Holevo, *Statistical Structure of Quantum Theory*, Lect. Not. Phys **61**, (Springer, Berlin, 2001).
- ¹⁸ S. L. Braunstein, C. M. Caves, Phys. Rev. Lett. **72** 3439 (1994); S. L. Braunstein, C. M. Caves, G. J. Milburn, Ann. Phys. **247**, 135 (1996).
- ¹⁹ A. Fujiwara, METR **94-08** (1994).
- ²⁰ S. Amari and H. Nagaoka, *Methods of Information Geometry*, Trans. Math. Mon. **191**, AMS (2000).
- ²¹ M. G A Paris, Int. J. Quant. Inf. **7**, 125 (2009).
- ²² P. Zanardi, M. G. A. Paris, L. Campos Venuti, Phys. Rev. A **78**, 042105 (2008).
- ²³ M. Tsang, Phys. Rev. A **88**, 021801(R) (2013).
- ²⁴ G. Salvatori, A. Mandarino, M. G. A. Paris, Phys. Rev. A, **90**, 022111 (2014).
- ²⁵ M. Bina, I. Amelio, M. G. A. Paris, preprint arXiv:1601.04015
- ²⁶ H. Cramer, *Mathematical methods of statistics*, (Princeton University Press, 1946).
- ²⁷ F. Troiani, A. Ghirri, M. Affronte, S. Carretta, P. Santini, G. Amoretti, S. Piligkos, G. Timco, and R. E. P. Winpenny, Phys. Rev. Lett., **94**, 207208 (2005).
- ²⁸ I. Siloi and F. Troiani, Phys. Rev. B, **86**, 224404 (2012).